Published in final edited form as:

*Anal Chim Acta*. 2004 September 20; 522(1): 9–17. doi:10.1016/j.aca.2004.06.040.

# Fluorescence intensity and lifetime-based cyanide sensitive probes for physiological safeguard

**Ramachandram Badugu**[a], **Joseph R. Lakowicz**[a], **Chris D. Geddes**[a,b,*]

[a]Center for Fluorescence Spectroscopy, Department of Biochemistry and Molecular Biology, Medical Biotechnology Center, University of Maryland School of Medicine, 725 West Lombard Street, Baltimore, MD 21201, USA

[b]Institute of Fluorescence and Center for Fluorescence Spectroscopy, Medical Biotechnology Center, University of Maryland Biotechnology Institute, 725 West Lombard Street, Baltimore, MD 21201, USA

## Abstract

We characterize six new fluorescent probes that show both intensity and lifetime changes in the presence of free uncomplexed aqueous cyanide, allowing for fluorescence based cyanide sensing up to physiological safeguard levels, i.e. <30 μM. One of the probes, *m*-BMQBA, shows a ≈15-fold reduction in intensity and a ≈10% change in mean lifetime at this level.

The response of the new probes is based on their ability to bind the cyanide anion through a boronic acid functional group, changing from the neutral form of the boronic acid group R–$B(OH)_2$ to the anionic R–$B^-(CN)_3$ form, a new cyanide binding mechanism which we have recently reported. The presence of an electron deficient quaternary heterocyclic nitrogen nucleus, and the electron rich cyanide bound form, provides for the intensity changes observed. We have determined the disassociation constants of the probes to be in the range ≈ 15–84 $\mu M^3$. In addition we have synthesized control compounds which do not contain the boronic acid moiety, allowing for a rationale of the cyanide responses between the probe isomers to be made.

The lifetime of the cyanide bound probes are significantly shorter than the free R–$B(OH)_2$ probe forms, providing for the opportunity of lifetime based cyanide sensing up to physiologically lethal levels.

Finally, while fluorescent probes containing the boronic acid moiety have earned a well-deserved reputation for monosaccharide sensing, we show that strong bases such as $CN^-$ and $OH^-$ preferentially bind as compared to glucose, enabling the potential use of these probes for cyanide safeguard and determination in physiological fluids, especially given that physiologies do not experience any notable changes in pH.

### Keywords

Cyanide sensing; Boronic acid; Fluorescence sensing; Poison; Physiological safeguard; Lifetime-based sensing

*Corresponding author. chris@cfs.umbi.umd.edu (C.D. Geddes).

## 1. Introduction

Cyanide has long been known to be a toxic substance, the toxicity of its salts exploited for many hundreds of years. It was not until 1782 that cyanide itself was identified, isolated by the Swedish Chemist Scheele, who later himself died from cyanide poisoning [1]. More recently cyanide was unsuccessfully used as a chemical warfare agent in World War 1, primarily because of the way it was delivered [1], and is also thought to have been used against the inhabitants of the Kurdish city of Hama, Iraq [2], and in Shahabad, Iran, during the Iran–Iraq war [3]. Based on recent cyanide history, acute cyanide poisoning continues to constitute a threat for military forces in future conventional and unconventional conflicts [1].

Cyanide is also readily used in industry in the making of plastics, in the recovery of gold and silver from ores, and in the electroplating of metals, such as silver, gold, platinum and copper [1]. However, while cyanide is used in both military and industrial applications, cyanide poisoning is not common, but can more surprisingly occur from smoke inhalation from residential and industrial fires [1,4,5], where the combustion of synthetic products that contain carbon and nitrogen, such as plastics and synthetic fibers, release cyanide. Cigarette smoke also contains cyanide, the nonsmoker typically averages about 0.06 μg/mL (2.31 μM) of cyanide in blood, where as a smoker typically averages 0.17 μg/mL (6.5 μM) [6].

The mechanism of cyanide poisoning is by absorption, through the GI track, skin and lungs. Cyanide's toxicity lies in its ability to inhibit oxygen utilization by cells, binding to the active site of cytochrome oxidase [7,8], hence, the tissues with the highest oxygen requirement (brain, heart and lungs) are the most affected by acute poisoning. There have been numerous studies of fire victims to asses the lethal levels of cyanide [1,4,5,9]. Fire survivors have been found to have <20 μM cyanide in blood, while victims were found to have levels greater than ≈20–30 μM and in some cases as much as 100 μM cyanide [1,9]. The estimated intravenous dose that is lethal to 50% of the exposed population ($LD_{50}$) of HCN for a man is 1.0 mg/kg, and the estimated $LD_{50}$ for liquid on the skin is about 100 mg/kg [1]. Hence, any cyanide monitoring analytical technique would need a cyanide dynamic range from only few μM to <30 μM to ensure *physiological safeguard*.

Numerous chemical and physiochemical methods for the detection and determination of free aqueous cyanides, such as potentiometric, chromatographic, spectrophotometric, flow injection and electrochemical analysis, to name but just a few, are able to detect physiologically important cyanide levels [10–14], but most of these systems are not cheap, portable and indeed field deployable, most requiring the benefits of an analytical laboratory [10–14].

However, it is well recognized that fluorescence techniques for sensing, such as lifetime, intensity and wavelength ratiometric sensing [15–17] offer many advantages in the development of miniaturized, cheap, remote, accurate and precise sensors for both laboratory and environmental sensing [15–17]. However, one constraint with fluorescence based cyanide sensing to date, has been the development of suitable probes that show appropriate changes in their fluorescent properties in the 0–30 μM cyanide concentration range.

In this paper, we characterize six new boronic acid containing fluorophores, Fig. 1 (BAFs), which show both notable intensity and lifetime changes with <30 μM free aqueous cyanide. In addition we have synthesized two control compounds which allow the sensing mechanism and contribution from dynamic quenching to be also realized.

## 2. Experimental

### 2.1. Materials

All chemicals were purchased from Sigma. The preparation of the *ortho*, *meta* and *para* forms of BMQBA, BMO-QBA and the control compounds BMQ and BMOQ, Fig. 1, have recently been reported by us [19,20]. The response of our new probes is based on the ability of the boronic acid group to interact with the uncomplexed $CN^-$ anion, displacing the hydroxyl ion, changing from the neutral form of the boronic acid to the anionic $R–B^-(CN)_3$ form, Scheme 1, which in turn interacts with an electron deficient (positively charged) quaternary heterocyclic nitrogen center. We have recently reported this new cyanide sensing mechanism, with regard to a wavelength ratiometric probe, which saturated at about 20 μM cyanide [18]. The new probes reported here, have much broader dynamic sensing ranges and benefit from the advantages of fluorescence lifetime based sensing [15–17].

### 2.2. Methods

Fluorescence spectra were collected on a Varian Eclipse spectrofluorometer with solution optical densities less than 0.2 and $\lambda_{ex}$ = 345 and 320 nm for BMOQBA and BMQBA, respectively. The probe concentration used throughout this study was ≈5 μM, noting that the binding of the probe and free cyanide is indeed an equilibrium, Scheme 1.

Stability ($K_S$—units $\mu M^{-3}$ or $mol^{-3}\ dm^9$ for $CN^-$ and $mM^{-1}$ or $mol^{-1}\ dm^3$ for glucose and fructose) and dissociation constants ($K_D$) were obtained by fitting the titration curves with aqueous sodium cyanide to the relation:

$$I = \frac{I_{min} + I_{max} K_S[\text{cyanide}]}{1 + K_S[\text{cyanide}]} \quad (1)$$

where $I_{min}$ and $I_{max}$ are the initial (no cyanide) and final (plateau) fluorescence intensities of the titration curves, where $K_D = (1/K_S)$.

Time-resolved intensity decays were measured using reverse start-stop time-correlated single-photon counting (TC-SPC) [15] with a Becker and Hickl gmbh 630 SPC PC card and an un-amplifed MCP-PMT. Vertically polarized excitation at ≈372 nm was obtained using a pulsed LED source (1 MHz repetition rate) and a dichroic sheet polarizer. The instrumental response function was ≈1.1 ns fwhm. The emission was collected at the magic angle (54.7°), using a long pass filter (Edmund Scientific), which cut off wavelengths below 416 nm.

The intensity decays were analyzed in terms of the multiexponential model [15]:

$$I(t) = \sum_i \alpha_i \exp(-t/\tau_i) \quad (2)$$

where $\alpha_i$ are the amplitudes and $\tau_i$ the decay times, $\sum \alpha_i = 1.0$. The fractional contribution of each component to the steady-state intensity is given by:

$$f_i = \frac{\alpha_i \tau_i}{\sum_i \alpha_i \tau_i} \quad (3)$$

The mean lifetime of the excited state is given by:

$$\bar{\tau} = \sum_i f_i \tau_i \quad (4)$$

and the amplitude-weighted lifetime is given by:

$$\langle \tau \rangle = \sum_i \alpha_i \tau_i \quad (5)$$

The values of $\alpha_i$ and $\tau_i$ were determined by non-linear least squares impulse reconvolution with a goodness-of-fit $\chi^2 R$ criterion [15].

Steady-state and time-resolved (lifetime) based Stern–Volmer constants were obtained using the well-known Stern–Volmer relationship [17]:

$$\frac{I'}{I} = \frac{\tau_0}{\tau} = 1 + K_{SV}[\text{Cyanide}] \quad (6)$$

where $I'$ and $\tau_0$ are the intensities and lifetimes in the absence of cyanide respectively, and $K_{SV}$ is the Stern–Volmer constant, $M^{-1}$. For detailed descriptions and applications of the Stern–Volmer relation, see [15,17] and references therein.

The quantum yield values were determined from a spectral comparison with *N*-(3-sulfopropyl)-6-methoxyquinolinium, where $\phi_f = 0.53$ in water [15,17].

## 3. Results

### 3.1. Fluorescence intensity-based cyanide sensing

Fig. 2 shows the absorption and emission spectra of *o*-BMOQBA and *o*-BMQBA in water, where the spectra are representative of the other respective isomers shown in Fig. 1. The *o*-BMOQBA shows an ≈100 nm Stokes-shifted fluorescence band at 450 nm, while the BMQBAs show ≈120 nm. The differences in the absorption spectra can be attributed to the n $\rightarrow \pi^*$ absorption band of the methoxy oxygen in the six-position on the quinoline backbone. The large Stokes shifts for these probes is ideal for fluorescence sensing, providing for the both an easy discrimination between excitation and observation wavelengths, and the possible use of LED's as cheap excitation sources, which are well-known to be both

spectrally and temporally broad [15]. In this regard we have been able to use a 372 nm pulsed LED for our time-resolved studies, described later.

Fig. 3 shows the emission spectra of the three BMO-QBA isomers for increasing cyanide concentrations, with $\lambda_{ex}$ = 345 nm. As the cyanide concentration increases monotonically to a maximum value of 100 μM, the emission band at 450 nm decreases. For the control compound, BMOQ, we typically observed only a very slight decrease in emission intensity for increasing cyanide concentrations, which we have attributed to dynamic fluorescence quenching (see lifetime data) by cyanide, Fig. 4(top), noting that BMOQ does not possess a boronic acid group and therefore can not bind cyanide as postulated in our recent reports [18,21]. By plotting the intensity of BMOQ in the presence of cyanide, normalized by the intensity in the absence of cyanide, we were subsequently able to determine the Stern–Volmer quenching constant to be ≈3000 $M^{-1}$, cf. Eq. (6).

For the data shown in Fig. 3 we were able to construct intensity ratiometric type plots, i.e. the intensity in the absence of cyanide divided by the intensity in the presence of cyanide, Fig. 5. Interestingly the *m*-BMOQBA isomer shows a much stronger response to cyanide with a 10-fold intensity change with as little as 20 μM cyanide. Using Eq. (1) and the data in Fig. 5, we were able to determine the cyanide dissociation constants for the *ortho*, *meta* and *para* boronic acid probes to be 52.9, 84.0 and 20.8 $\mu M^3$, noting the units $\mu M^3$ or $mol^3\ dm^{-9}$ based on the equilibrium shown in Scheme 1. These responses are most encouraging and suggest the use of these isomers for physiological cyanide safeguard. In addition, *m*-BMOQBA may find applications for cyanide determination post-mortem for fire victims, where cyanide levels exceed the ≈20 μM lethal concentration threshold [1,4,5,9].

To understand the different responses of the isomers towards cyanide it is informative to consider the charge neutralization–stabilization mechanism of these probes, which we have recently reported for glucose [19,20,22]. Upon binding and displacement of the hydroxyl ion, the electron density on the boron atom of the probe is increased, Scheme 1, facilitating the partial neutralization of the positively charged quaternary nitrogen of the quinolinium moiety. The quaternary nitrogen not only reduces the p$K_a$ of the probe [19,20], but also stabilizes the boronate–cyanide complex formed upon cyanide addition. The differences in cyanide sensitivity between the isomers is explained by either their throughspace or through–bound interactions [23,24] with the positively charged nitrogen, the *meta* form of the probes thought to interact via both mechanisms [23,24].

Fig. 6 shows the emission spectra for the BMQBA probes and the control compound BMQ for increasing cyanide concentrations. Similarly to the BMOQBA probes, the BMQBA probes show a notable decrease in fluorescence intensity with μM cyanide concentrations. BMQ is however relatively unperturbed, with a Stern–Volmer constant smaller than for BMOQ, Fig. 4, ≈800 $M^{-1}$. We again plotted the intensity ratiometric type plots for the data shown in Fig. 6. Fig. 7 shows an ≈12-fold decrease in fluorescence intensity with 30 μM cyanide for *m*-BMQBA, ideal for free uncomplexed cyanide physiological safeguard monitoring, with dissociation constants $K_D$ of 16.7, 16.9 and 15.9 $\mu M^3$ for the *ortho*-, *meta*- and *para*-forms, respectively. Interestingly the response of *m*-BMOQBA shows twice the response with 75 μM cyanide as compared to the *m*-BMQBA probe. We have attributed this

notable difference to the difference in electron donating capabilities between the methyl and methoxy groups in the six-position on the quinolinium backbone and the resultant charge on the quaternary nitrogen heterocyclic center. This is also reflected in the quantum yields of the probes, with *m*-BMOQBA having a quantum yield of 0.51 as compared to 0.025 for *m*-BMQBA.

### 3.2. Fluorescence lifetime-based cyanide sensing

With notable changes in the fluorescence intensities of the probes in the presence of cyanide we questioned whether changes in the mean lifetime of the probe would also provide for lifetime based sensing. Our reasoning was based on our recent report of a similar probe, based on the 6-amino quinoline nucleus, which showed both spectral shifts and intensity changes in the presence of cyanide, allowing for both excitation and emission wavelength-ratiometric cyanide sensing [18]. The dual emission bands enabled us previously to clearly resolve the lifetime of both the cyanide bound and unbound probe forms where we concluded that the bound form had a much shorter lifetime, a few hundred ps, in comparison to the unbound form which had a mean lifetime of 2.59 ns. We have subsequently measured the lifetimes of the new probes using the well-known time-correlated single photon timing technique, TCSPC [15], a representative isomer shown in Tables 1 and 2.

The lifetime of *o*-BMOQBA was found to be monoexponential in water with a lifetime of 26.71 ns, Table 1. However, in the presence of cyanide the intensity decay is biexponential with a much shorter component now present, ≈300–450 ps. This has the result of reducing the mean lifetime by 4–8% over the range of physiological cyanide importance. Interestingly these measurements were undertaken with a pulsed UV LED with an emission centered at 372 nm, suggesting the utility of the new probes for potential use in low power, field-deployable poison safeguard devices. Similar findings were observed for the other isomers.

The lifetime of the control compound BMOQ is monoexponential both in water and in the presence of cyanide, decreasing from 27.30 → 25.0 ns with up to 50 μM cyanide. In comparison, the lifetime of *o*-BMOQBA in water was found to be slightly shorter, 26.71 ns. Using Eq. (6) we calculated the dynamic quenching Stern–Volmer constant to be ≈1840 $M^{-1}$, similar to the value obtained from the intensity-based measurements shown in Fig. 4. We subsequently assign the decrease in fluorescence intensity shown in Fig. 4(top), to dynamic fluorescence quenching by cyanide. Interestingly the presence of a much shorter lifetime component for *o*-BMOQBA with cyanide, suggests more than a simple collisional quenching process is present. Given this, and the fact that the intensity rapidly decreases in the presence of cyanide, it seems logical that the cyanide bound probe has both a short lifetime, and a significantly reduced quantum yield as compared to the unbound probe form.

Table 2 shows the intensity decay kinetics of BMQ and *o*-BMQBA. The control compound BMQ was found to be monoexponential in water with a lifetime of 2.59 ns. The presence of cyanide results in a slight decrease in the life-time, the Stern–Volmer quenching constant ≈314 $M^{-1}$, not unlike that determined from the intensity plots, Figs. 4 and 6. The intensity decay of *o*-BMQBA was found to be biexponential in water, with the mean lifetime decreasing from 4.01 to 3.22 ns in the presence of 50 μM cyanide, a ≈25% change in mean lifetime which can not be explained by dynamic cyanide quenching, and is therefore

attributed to the cyanide bound form. In our analysis we recognize the complexity of assigning the cyanide bound lifetimes, as three possible bound probe forms are possible as shown in Scheme 1. Subsequently, we refer to all three bound forms as simply the cyanide bound form. Similar findings were observed for the other isomers also.

## 4. Discussion

It is widely accepted that ratiometric or lifetime based measurements offer some intrinsic advantages for biomedical fluorescence sensing [15,16]. The new probes characterized in this paper have the advantage of showing both intensity and lifetime based changes to physiologically important cyanide concentrations, both sets of probes bringing new advantages to our arsenal of fluorescent probes for cyanide determination.

The BMOQBA's typically display a greater dynamic range for sensing, with notable changes observed in the cyanide concentration range 5–60 μM. The BMOQBA's are highly water-soluble and can be prepared in a one step synthesis [20]. The ≈350 nm absorption band readily allows for UV LED excitation or even 370 nm/400 nm laser diode excitation, which would not be possible with the BMQBA's Fig. 2. The long lifetime of the BMOQBA's (≈26 ns) accounts for the more dramatic cyanide collisional quenching, also observed with the control compound BMOQ. Subsequently, these probes are likely to be susceptible to other interferences such as aqueous chloride or oxygen [15,17]. With regard to interferences by physiological monosaccharides, we have determined the dissociation constants of the *ortho*, *meta* and *para* forms to be 49.5, 1000 and 430 mM for glucose, and 0.65, 1.8 and 9.1 mM for fructose, respectively. Fructose, as expected, shows a greater affinity for the monophenyl boronic acid probes [25], but both sugars are not expected to interfere given the more efficient binding of cyanide.

The BMQBA probes also show notable changes in fluorescence intensity in the presence of 30 μM cyanide, 14- to 8-fold, for the *ortho* → *para* isomers, respectively. Unlike the BMOQBA probes, this class of probes shows a biexponential lifetime in water, and a relatively much shorter mean lifetime (4.01 ns) that typically decreases 25% with the addition of 50 μM cyanide. The lifetime reduction is thought to be due to the cyanide bound form, given the very minor changes observed with the control compound BMQ. Interestingly, these probes are not likely to be perturbed much by other collisional quenchers due to their short lifetimes. With regard to fluorescence lifetime sensing, these changes are readily detectable using simple and cheap instrumentation [15]. The dissociation constants of the *ortho*, *meta* and *para* forms of BMQBA were found to be 100, 476 and 370 mM for glucose, and 4.7, 13.2 and 13.8 mM, respectively, for fructose. One particular disadvantage of these probes however, is their requirement for UV excitation at 320 nm, which while possible with LEDs as shown here, to some degree limits their practical use in rapid analysis, portable, field deployable devices.

Finally, it is informative to consider other probes we have recently developed for cyanide sensing also based on the quinolinium nucleus, which serves to directly compliment these findings. By replacing the 6-methoxy or 6-methyl groups with a more efficient electron donating group, such as an amino group, it is possible to observe dual emission bands from

both the free and cyanide complexed forms. This has enabled both colorimetric and ratiometric cyanide sensing, where the probe saturated at about 20 μM cyanide [18]. Interestingly, solutions of *o*-BAQBA showed useful color changes from green (Safe) to completely colorless (Danger) by the addition of 20 μM cyanide. However, the mean lifetime changes were small, precluding this probe from lifetime based cyanide sensing [18]. It is also interesting to note that probes synthesized with either a *nitro* or *chloro*-group in the six-position on the quinolinium backbone, had very low quantum yields and were not practical for sensing. Hence, it is possible to develop probes for cyanide, utilizing different fluorescence sensing methodologies such as lifetime, intensity or wavelength ratiometric, by simply using different substituents on the quinolinium heterocyclic backbone and/or different phenyl boronic isomers.

## 5. Conclusions

We have characterized six new fluorescent probes that show both intensity and lifetime changes in the presence of aqueous cyanide. All six probes show between a 5- and 15-fold reduction in fluorescence intensity, and one class of probes show up to a 25% change in mean lifetime in the presence of 30 μM cyanide. By characterizing two additional control compounds, BMQ and BMOQ which do not contain the boronic acid moiety and therefore do not bind cyanide, we have been able to further rationale and support the cyanide binding mechanism [18,21], as well as account for the dynamic quenching component in the cyanide response.

The relatively higher binding constants (smaller dissociation constants) for cyanide as compared to glucose and fructose, strongly suggest the use of these probes for cyanide sensing and/or physiological safeguard.

## Acknowledgements

This work was supported by the National Center for Research Resources, RR-08119. Partial salary support to JRL and CDG from UMBI is also gratefully acknowledged.

## Abbreviations:

| | |
|---|---|
| **BA** | boronic acid |
| **BAF and BAFs** | boronic acid containing fluorophore/s |
| **o-BAQBA** | *N*-(2-boronobenzyl)-6-aminoquinolinium bromide |
| ***o, m, p*-BMOQBA** | *N*-(2, 3 or 4-boronobenzyl)-6-methoxyquinolinium bromide |
| **BMQ** | *N*-benzyl-6-methoxyquinolinium bromide |
| ***o, m, p*-BMQBA** | *N*-(2,3,4-boronobenzyl)-6-methylquinolinium bromide |
| **BMQ** | *N*-benzyl-6-methylquinolinium bromide |
| $K_{SV}$ | Stern–Volmer quenching constant |

| | |
|---|---|
| **LD** | laser diode |
| **$LD_{50}$** | lethal dose to 50% of the population |
| **LED** | light emitting diode |
| **PET** | photoinduced electron transfer |
| **TCSPC** | time-correlated single photon counting |

## References


[1]. Baskin SI, Brewer TG, in: Sidell F, Takafuji ET, Franz DR (Eds.), Medical Aspects of Chemical and Biological Warfare, TMM publications, Washington, 1997, pp. 271–286 (Chapter 10).

[2]. Lang JS, Mullin D, Fenyvesi C, Rosenberg R, Barnes J, US News & World Report, vol. 10, 11 1986, p. 29.

[3]. Medical expert reports use of chemical weapons in Iran–Iraq war, UN Chronicle 22 (1985) 24–26.

[4]. Ishii A, Seno H, Watanabe-Suzuki K, Suzuki O, Kumazawa T, Anal. Chem 70 (22) (1998) 4873–4876. [PubMed: 9844576]

[5]. Moriva F, Hashimoto Y, J. For. Sci 46 (6) (2001) 1421–1425.

[6]. Clark CJ, Campbell D, Reld WH, Lancet i (1981) 1332–1335.

[7]. Warburg O, Hoppe-Seyler's Z Physiol. Chem 76 (1911) 331–346.

[8]. Kellin D, Proc. R. Soc. Lond. B. Biol. Sci 104 (1929) 206–251.

[9]. Baud FJ, Barriot P, Toffis V, N. Engl. J. Med 325 (1991) 1761–1766. [PubMed: 1944484]

[10]. Giuriati C, Cavalli S, Gorni A, Badocco D, Pastore P, J. Chromatogr. A 1023 (2004) 105–112. [PubMed: 14760854]

[11]. Beck HP, Zhang B, Bordeanu A, Anal. Lett 36 (2003) 2211–2228.

[12]. Fernandez-Arguelles MT, Costa-Fernandez JMC, Pereiro R, Sanz-Medel A, Anal. Chim. Acta 491 (2003) 27–35.

[13]. Deep B, Balasubramanian N, Nagaraja KS, Anal. Lett 36 (2003) 2865–2874.

[14]. Favero JAD, Tubino M, Anal. Sci 19 (2003) 1139–1143. [PubMed: 12945666]

[15]. Lakowicz JR, Principles of Fluorescence Spectroscopy, second ed., Kluwer/Academic Plenum publishers, New York, 1997.

[16]. Gryczynski Z, Gryczynski I, Lakowicz JR, Fluorescence sensing methods, Meth. Enzymol 360 (2002) 44–75.

[17]. Geddes CD, Meas. Sci. Technol 12 (9) (2001) R53–R88.

[18]. Badugu R, Lakowicz JR, Geddes CD, Anal. Biochem 327 (1) (2004) 82–90. [PubMed: 15033514]

[19]. Badugu R, Lakowicz JR, Geddes CD, Talanta, in press.

[20]. Badugu R, Lakowicz JR, Geddes CD, Bioorg. Med. Chem, submitted for publication.

[21]. Badugu R, Lakowicz JR, Geddes CD, Dyes and Pigments, in press.

[22]. Badugu R, Lakowicz JR, Geddes CD, J. Fluoresc 13 (2003) 371–374. [PubMed: 27340364]

[23]. Fox MA, Chanon M (Eds.), Photoinduced Electron Transfer, El-seveier, New York, 1998 (Part A–D).

[24]. Kavarnos GJ, Fundamentals of Photoinduced Electron Transfer, VCH, New York, 1993.

[25]. Dicesare N, Lakowicz JR, J. Biomed. Opt 7 (4) (2002) 538–545. [PubMed: 12421119]

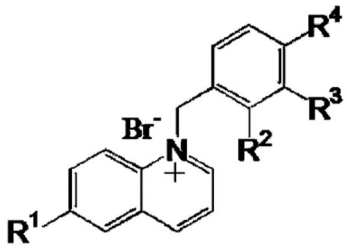


| Probe | $R^1$ | $R^2$ | $R^3$ | $R^4$ |
|---|---|---|---|---|
| *o*-BMOQBA | $OCH_3$ | $B(OH)_2$ | H | H |
| *m*-BMOQBA | $OCH_3$ | H | $B(OH)_2$ | H |
| *p*-BMOQBA | $OCH_3$ | H | H | $B(OH)_2$ |
| BMOQ | $OCH_3$ | H | H | H |
| *o*-BMQBA | $CH_3$ | $B(OH)_2$ | H | H |
| *m*-BMQBA | $CH_3$ | H | $B(OH)_2$ | H |
| *p*-BMQBA | $CH_3$ | H | H | $B(OH)_2$ |
| BMQ | $CH_3$ | H | H | H |

**Fig. 1.**

Molecular structure of the *ortho*, *meta* and *para*-BMOQBA and BMQBA probes and the respective control compounds BMOQ and BMQ, which do contain the boronic acid functional group.

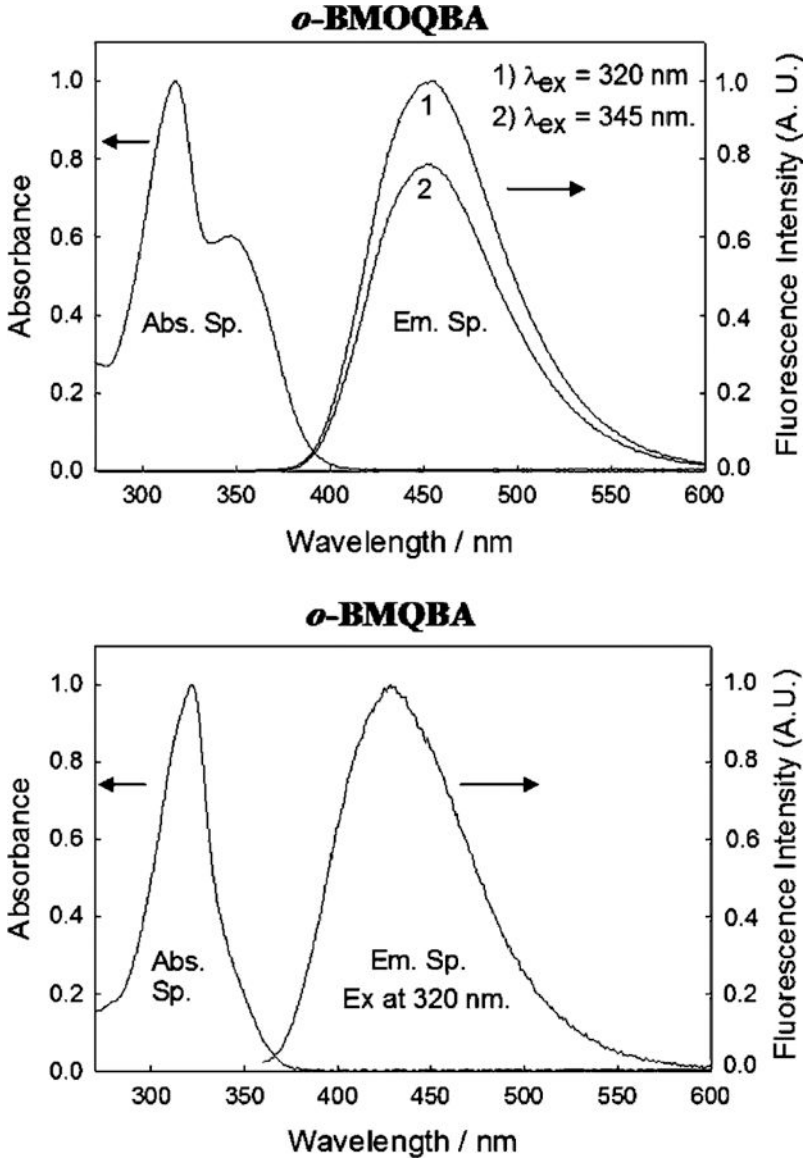


**Fig. 2.**

Absorption and emission spectra of aqueous *o*-BMOQBA and *o*-BMQBA. The spectra are representative of the other respective isomers.

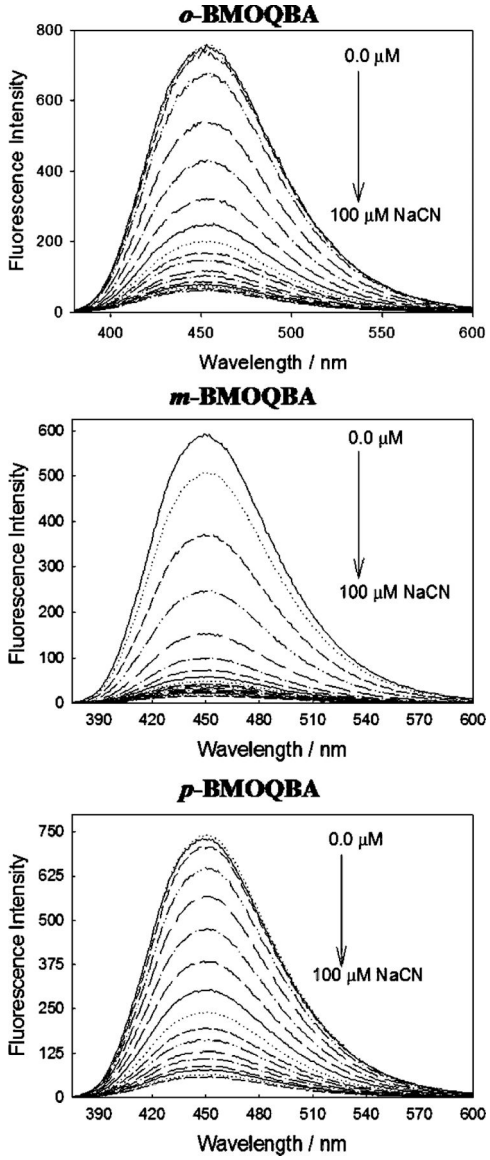


**Fig. 3.**

Emission spectra of *o*, *m*, *p*-BMOQBA in the presence of increasing cyanide concentrations. $\lambda_{ex}$ = 345 nm.

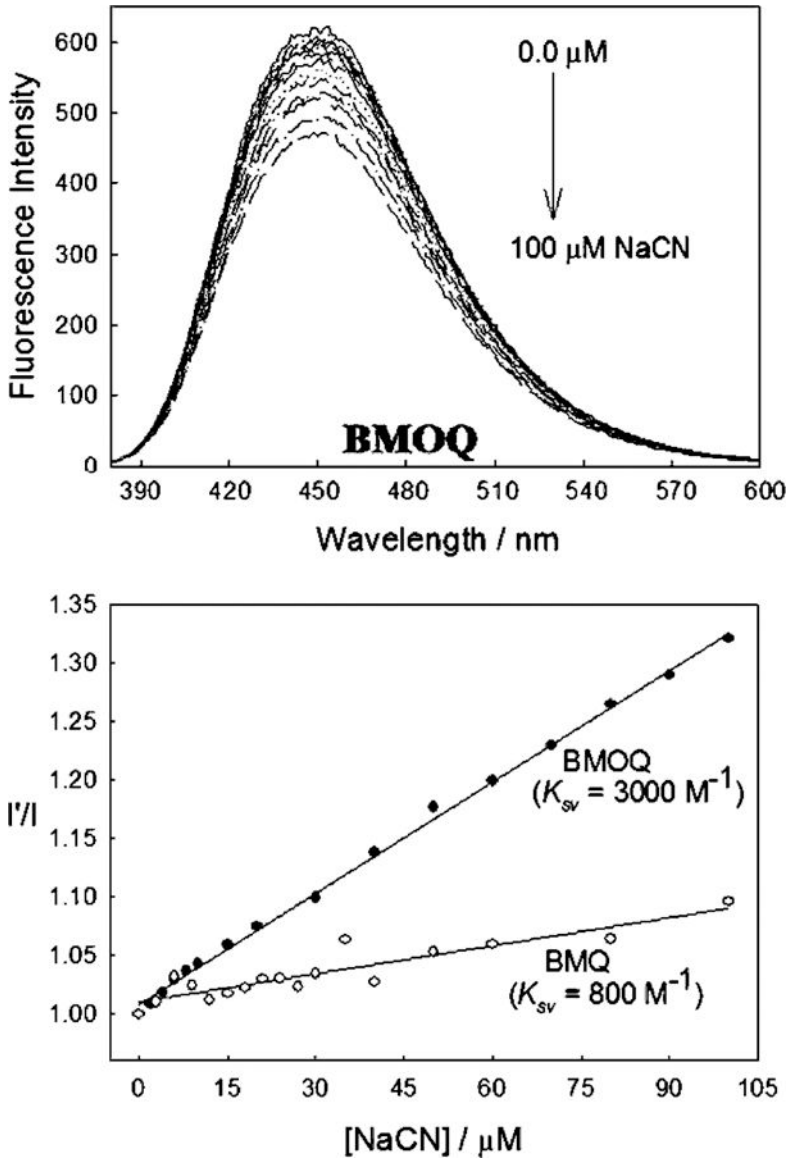


**Fig. 4.**

Emission spectrum of the control compound BMOQ with increasing cyanide concentrations (top), ($\lambda_{ex}$ = 345 nm) and the respective Stern–Volmer like plots for both BMOQ and BMQ, where $I'$ and $I$ are the fluorescence intensities at 450 nm in the absence and presence of cyanide, respectively (bottom).

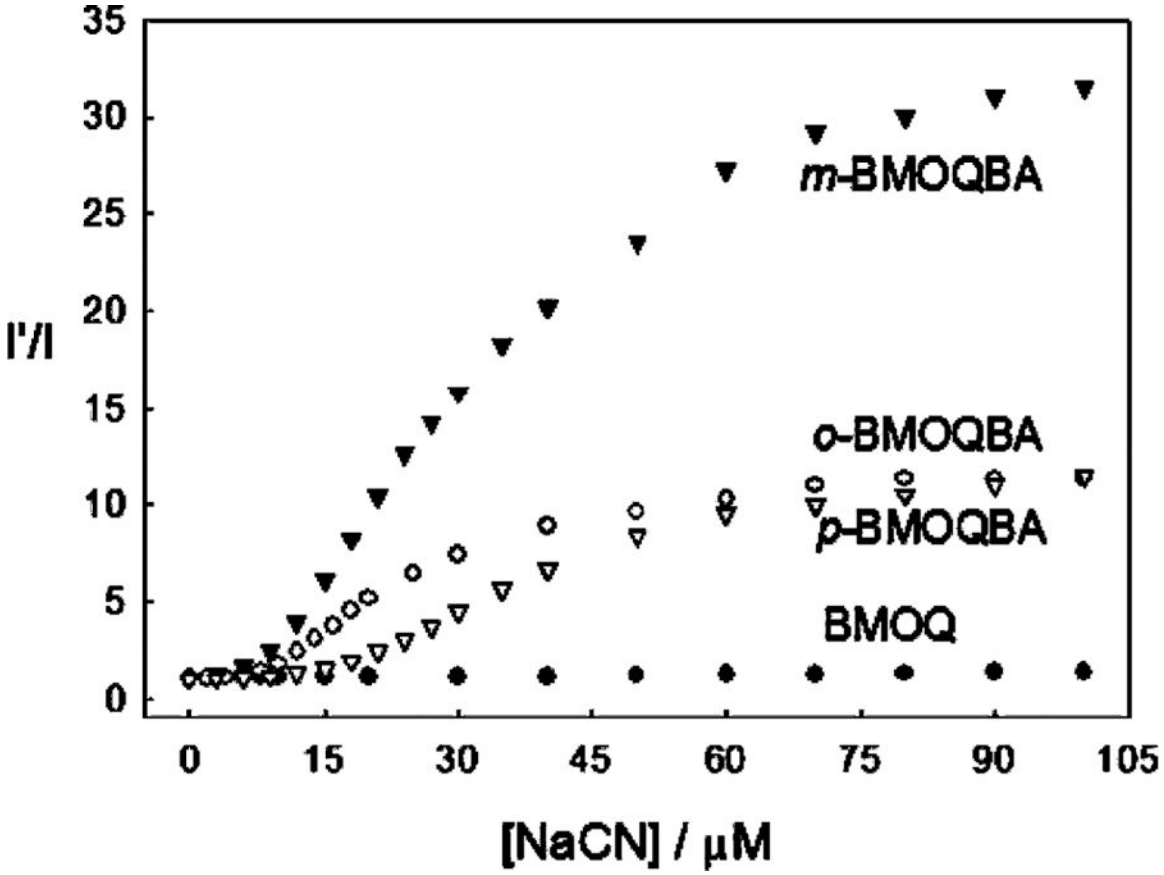


**Fig. 5.**

The response of the BMOQBA probes and BMOQ towards aqueous cyanide, where $I'$ and $I$ are the fluorescence intensities at 450 nm in the absence and presence of cyanide, respectively.

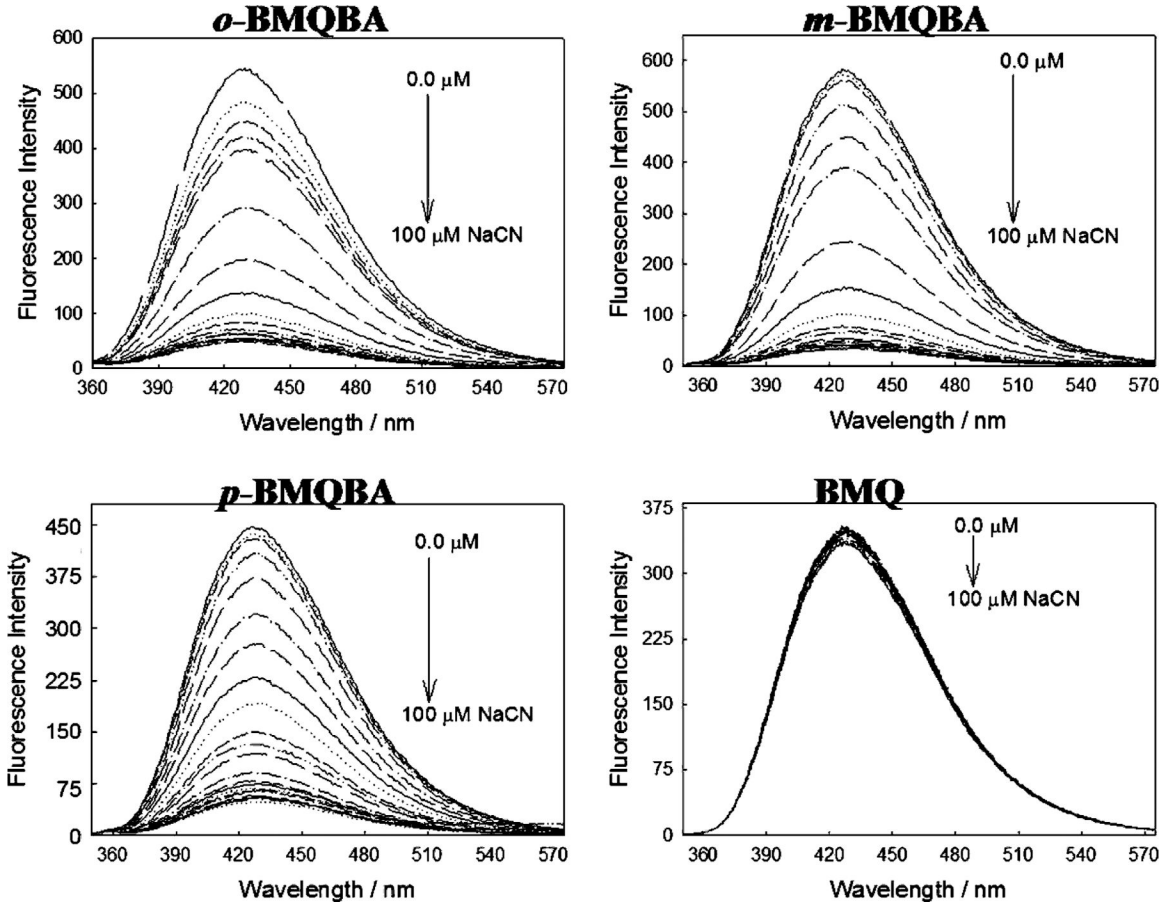


**Fig. 6.**

Emission spectra of *o*, *m*, *p*-BMQBA and the control compound BMQ, in the presence of increasing cyanide concentrations. $\lambda_{ex}$ = 320 nm.

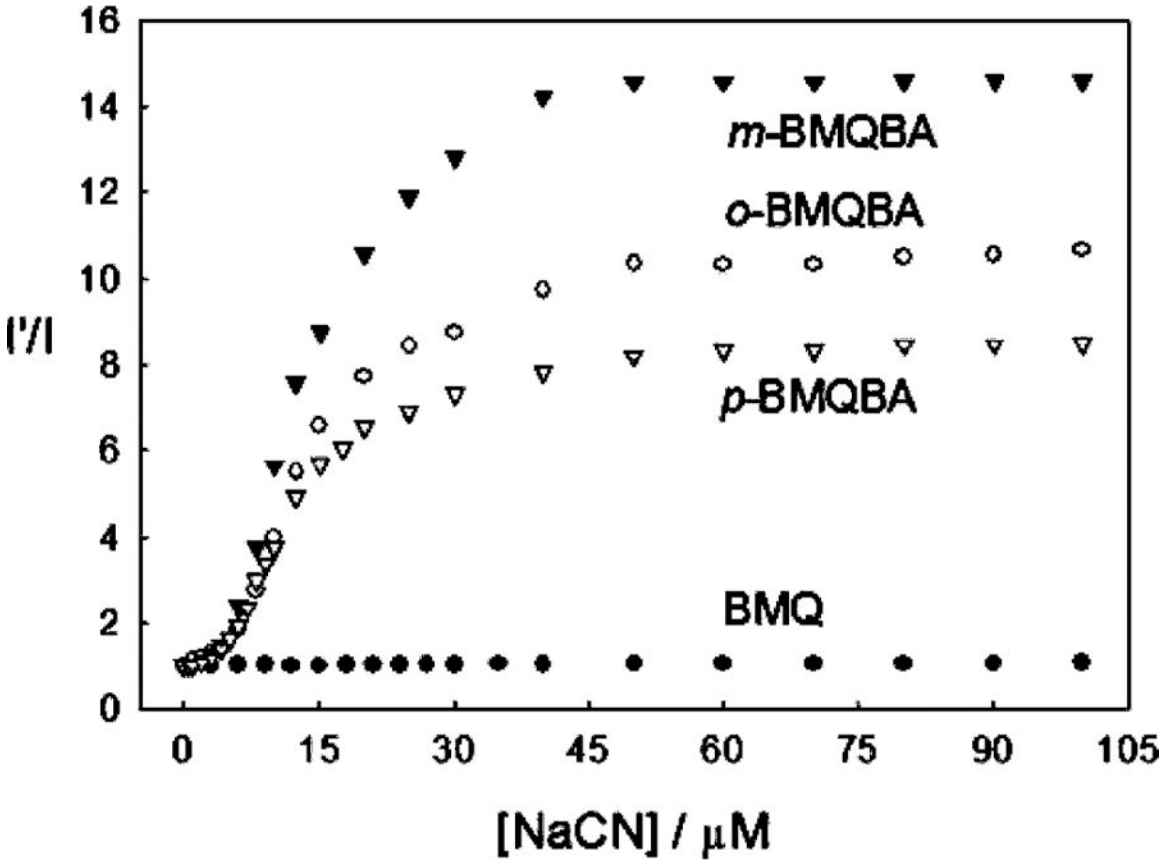


**Fig. 7.**

The response of the BMQBA probes and BMQ towards aqueous cyanide, where $I'$ and $I$ are the fluorescence intensities at 450 nm in the absence and presence of cyanide, respectively.

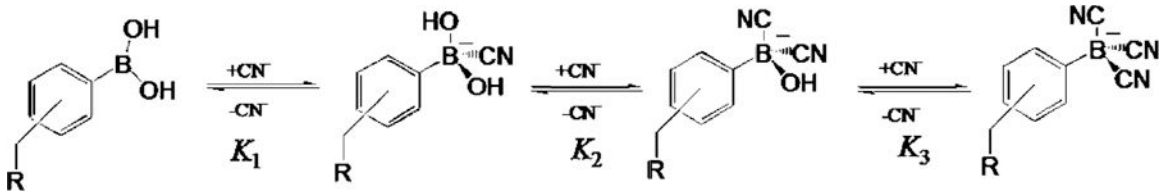


**Scheme 1.**

Equilibrium involved in the interaction between the boronic acid group and cyanide.

**Table 1**

Multiexponential Intensity decay of BMOQ and *o*-BMOQBA

| Compound | [$CN^-$] (μM) | $\tau_1$ (ns) | $\alpha_1$ | $\tau_2$ (ns) | $\alpha_2$ | $\bar{\tau}$(ns) | $\langle\tau\rangle$(ns) | $\chi^2$ |
|---|---|---|---|---|---|---|---|---|
| *o*-BMOQBA[a] | 0 | 26.71 | 1.0 | – | – | 26.71 | 26.71 | 1.33 |
| | 5 | 26.33 | 1.0 | – | – | 26.33 | 26.33 | 1.13 |
| | 10 | 26.34 | 1.0 | – | – | 26.34 | 26.34 | 1.21 |
| | 15 | 26.19 | 1.0 | – | – | 26.19 | 26.19 | 1.30 |
| | 25 | 24.78 | 1.0 | – | – | 24.78 | 24.78 | 1.23 |
| | 35 | 0.324 | 0.0160 | 25.54 | 0.9840 | 25.53 | 25.14 | 1.35 |
| | 45 | 0.326 | 0.0184 | 25.10 | 0.9816 | 25.09 | 24.64 | 1.46 |
| | 50 | 0.455 | 0.0176 | 25.20 | 0.9824 | 25.19 | 24.76 | 1.41 |
| BMOQ[a] | 0 | 27.30 | 1.0 | – | – | 27.30 | 27.30 | 1.08 |
| | 5 | 27.04 | 1.0 | – | – | 27.04 | 27.04 | 1.10 |
| | 10 | 26.74 | 1.0 | – | – | 26.74 | 26.74 | 1.12 |
| | 15 | 26.53 | 1.0 | – | – | 26.53 | 26.53 | 1.06 |
| | 20 | 26.25 | 1.0 | – | – | 26.25 | 26.25 | 1.14 |
| | 30 | 25.86 | 1.0 | – | – | 25.86 | 25.86 | 1.17 |
| | 40 | 25.37 | 1.0 | – | – | 25.37 | 25.37 | 1.05 |
| | 50 | 25.00 | 1.0 | – | – | 25.00 | 25.00 | 1.16 |

[a] $\lambda_{ex}$ = 372 nm, emission was collected with a 416 nm cut-off filter. BMOQ $K_{SV} \approx 1840\ M^{-1}$. The free columns indicate that the intensity decay was not described well by the addition of an extra decay time, $\tau_2$.

**Table 2**

Multiexponential intensity decay of BMQ and *o*-BMQBA

| Compound | [$CN^-$] (μM) | $\tau_1$ (ns) | $a_1$ | $\tau_2$ (ns) | $a_2$ | $\bar{\tau}$(ns) | $\langle\tau\rangle$(ns) | $\chi^2$ |
|---|---|---|---|---|---|---|---|---|
| *o*-BMQBA[a] | 0 | 2.18 | 0.4646 | 4.74 | 0.5354 | 4.01 | 3.55 | 1.00 |
| | 5 | 2.14 | 0.4615 | 4.45 | 0.5385 | 3.78 | 3.38 | 1.12 |
| | 10 | 2.28 | 0.5704 | 4.75 | 0.4296 | 3.78 | 3.34 | 1.04 |
| | 15 | 1.86 | 0.3265 | 3.64 | 0.6735 | 3.29 | 3.06 | 0.97 |
| | 20 | 1.88 | 0.3476 | 3.69 | 0.6524 | 3.30 | 3.06 | 1.04 |
| | 30 | 1.44 | 0.1762 | 3.27 | 0.8238 | 3.11 | 2.95 | 1.21 |
| | 40 | 1.92 | 0.3511 | 3.59 | 0.6489 | 3.21 | 3.00 | 0.90 |
| | 50 | 1.87 | 0.3320 | 3.58 | 0.6680 | 3.22 | 3.01 | 1.07 |
| BMQ[a] | 0 | 2.59 | 1.0 | – | – | 2.59 | 2.59 | 1.07 |
| | 5 | 2.58 | 1.0 | – | – | 2.58 | 2.58 | 1.09 |
| | 10 | 2.59 | 1.0 | – | – | 2.59 | 2.59 | 1.07 |
| | 15 | 2.57 | 1.0 | – | – | 2.57 | 2.57 | 1.02 |
| | 20 | 2.57 | 1.0 | – | – | 2.57 | 2.57 | 1.12 |
| | 30 | 2.55 | 1.0 | – | – | 2.55 | 2.55 | 1.08 |
| | 40 | 2.55 | 1.0 | – | – | 2.55 | 2.55 | 1.14 |
| | 50 | 2.55 | 1.0 | – | – | 2.55 | 2.55 | 1.17 |

[a] $\lambda_{ex}$ = 372 nm, emission was collected with a 416 nm cut-off filter. BMQ $K_{SV} \approx 314\ M^{-1}$. The free columns indicate that the intensity decay was not described well by the addition of an extra decay time, $\tau_2$.